



# International Operational Modal Analysis Conference

20 - 23 May 2025 | Rennes, France

## The ROTMAC Concept: An Experimental Application

Natalia García-Fernández<sup>1\*</sup>, Pelayo Fernández<sup>1</sup> and Manuel Aenlle<sup>1</sup>

<sup>1</sup> Department of Construction and Manufacturing Engineering, University of Oviedo, Gijón, Spain

\* garciafnatalia@uniovi.es

### ABSTRACT

Model correlation involves comparing two different models. When models exhibit closely spaced or repeated modes, small perturbations in mass or stiffness can cause significant rotations of the mode shapes within their local subspace. Consequently, when using the modal assurance criterion (MAC) to assess model correlation in such scenarios, low MAC values may be obtained in the case of significant angles of rotation, even when there is a strong correlation between the models in terms of mass and stiffness. To address this inconsistency, a variation of the MAC, termed ROTMAC, is proposed. The ROTMAC serves as an indicator of shear by computing the MAC after rotating the mode shapes of one of the systems. To obtain the rotation matrix  $R$ , the QR decomposition or the polar decompositions can be applied. In this study, the effectiveness of ROTMAC is demonstrated by analysing the correlation between different experimental structures with closely spaced modes and their corresponding numerical models. A square glass plate and two two-story lab-scale structures were considered in this study. The results show that ROTMAC successfully mitigates the effects of local rotations, leading to higher correlation values.

*Keywords: MAC, ROTMAC, Model correlation, Repeated modes, Closely spaced modes, Rotation.*

### 1. INTRODUCTION

When a system (denoted  $B$ ) is perturbed by a mass or stiffness change, mode shapes can exhibit rotation, shear and scaling variations, resulting in a perturbed system  $A$ . If two modes are considered, as shown in Fig. (1), shear occurs when the relative angle between modes differs between systems  $A$  and  $B$ . Pure rotation means that both modes rotate the same angle, i.e. the relative angle between modes is the same in systems  $A$  and  $B$ . Scaling refers to changes in the length of the mode shapes before and after the perturbation.

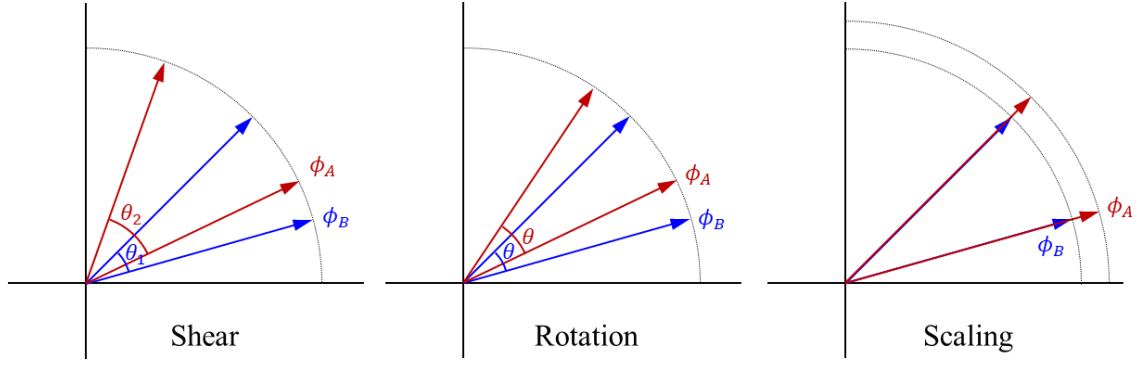


**Figure 1.** Data set used in the experiments.

In the case of closely spaced or repeated modes, even a small change in mass or stiffness can cause significant rotations in their local subspace, leading to low MAC values. Closely spaced or repeated modes typically appear in structures that present any type of symmetry such as towers, chimneys, buildings, etc. Therefore, two systems with strong correlation can present low MAC values due to local rotations. In this paper, the ROTMAC concept is proposed to eliminate the effects of rotation, ensuring that only shear discrepancies are detected.

## 2. THEORY

### 2.1. Structural dynamic modification theory

In this work, an unperturbed model B, defined by the mass matrix  $\mathbf{M}_B$  and the stiffness matrix  $\mathbf{K}_B$ , is considered. Model B is perturbed with the mass change matrix  $\Delta\mathbf{M}$  and the stiffness change matrix  $\Delta\mathbf{K}$ . According to the structural dynamic modification theory, the mass matrix of the modified (or perturbed) system  $\mathbf{M}_A$  can be expressed as:

$$\mathbf{M}_A = \mathbf{M}_B + \Delta\mathbf{M} \quad (1)$$

and the stiffness matrix  $\mathbf{K}_A$  as:

$$\mathbf{K}_A = \mathbf{K}_B + \Delta\mathbf{K} \quad (2)$$

The eigenvalue problem of the unperturbed system B is expressed as:

$$(\mathbf{K}_B - \mathbf{M}_B \omega_B^2) \boldsymbol{\phi}_B = 0 \quad (3)$$

where  $\omega_B^2$  is a diagonal matrix containing the squared numerical natural frequencies of system B. With respect to the perturbed system, the eigenvalue problem is given by:

$$(\mathbf{K}_A - \mathbf{M}_A \omega_A^2) \boldsymbol{\phi}_A = 0 \quad (4)$$

where  $\omega_A^2$  is a diagonal matrix containing the squared numerical natural frequencies of system A. According to the structural dynamic modification theory, it is derived that the modal matrix  $\boldsymbol{\phi}_A$  of the perturbed structure (usually the experimental model) can be expressed as a linear combination of the modal matrix of system  $\boldsymbol{\phi}_B$  (usually the numerical model) [1,2], as:

$$\boldsymbol{\phi}_A = \boldsymbol{\phi}_B \mathbf{T} \quad (5)$$

where  $\mathbf{T}$  is a transformation matrix. Considering that the response of the structure is only measured in a few degrees of freedom (DOFs) and only the modal parameters in a certain frequency range are identified, an estimation of matrix  $\mathbf{T}$  can be obtained by means of the expression [1,2]:

$$\mathbf{T} = \boldsymbol{\phi}_B^+ \boldsymbol{\phi}_A \quad (6)$$

where superscript '+' indicates pseudoinverse.

In the case of unscaled mode shapes for system A (denoted  $\boldsymbol{\psi}_A$ ), a new transformation matrix ( $\mathbf{T}_U$ ) is obtained as:

$$\mathbf{T}_U \approx \boldsymbol{\phi}_B^+ \boldsymbol{\psi}_A \quad (7)$$

### 2.1.1. Stiffness change

When a system B is only perturbed with a stiffness change [3] the following equation is derived:

$$\mathbf{I} = \mathbf{T}^T \mathbf{T} \quad (8)$$

From which it is inferred that matrix  $\mathbf{T}^T$  must be a rotation matrix, i.e.:

$$\mathbf{T}^T = \mathbf{R} \quad (9)$$

Therefore, in the case of stiffness discrepancies only rotation effects are present, and no shear or scaling effects appear.

### 2.1.2. Mass change

In the case of a system B only perturbed with a mass change, in addition to the rotation of the mode shapes, changes in the scaling and in the relative angle between the mode shapes (shear) also appear. Therefore, the matrix  $\mathbf{T}^T$  can be expressed as a linear combination of rotation ( $\mathbf{R}$ ), shear ( $\mathbf{T}_{sh}$ ) and scaling ( $\mathbf{T}_{sc}$ ) as:

$$\mathbf{T}^T = \mathbf{R} \mathbf{T}_{sh} \mathbf{T}_{sc} \quad (10)$$

Combining the effects of shear and scaling in just one matrix, Eq. (10) leads to:

$$\mathbf{T}^T = \mathbf{R} \mathbf{T}_{ch} \quad (11)$$

In the case of repeated modes, the effect of the perturbation is mainly a rotation of the mode shapes in their local subspace, together with changes in scaling. However, there is no effect of shear.

### 2.1.3. Decomposition of $\mathbf{T}^T$ matrix

Considering that a rotation is always involved in matrix  $\mathbf{T}$ , the QR decomposition [4] can be used to factorize matrix  $\mathbf{T}^T$  as:

$$\mathbf{T}^T = \mathbf{R} \mathbf{Q} \quad (12)$$

where matrix  $\mathbf{R}$  is a rotation matrix and  $\mathbf{Q}$  is an upper triangular matrix. The following results are expected in the following cases:

- In the case of only stiffness discrepancies ( $\Delta K$ ), matrix  $T^T$  is a pure rotation. Therefore, the  $Q$  matrix obtained with the QR decomposition will be an identity matrix in case of mass-normalized mode shapes, or a diagonal matrix in case of unscaled mode shapes.
- In the case of only mass discrepancies ( $\Delta M$ ), the QR decomposition gives a rotation matrix  $R$  and matrix  $Q$  containing information of shear and scaling.

Other decompositions can also be used to factorize the matrix  $T^T$  such as the polar decomposition.

## 2.2. ROTMAC

As previously explained, closely spaced modes are highly sensitive to small mass and stiffness perturbations of the system, and they can rotate within their subspace. Therefore, two models can present good correlation in terms of mass and stiffness, but still low MAC values can be obtained due to this rotation. Following these considerations, a new indicator, denoted as ROTMAC, is proposed.

The ROTMAC is a novel version of the MAC, where the rotated mode shapes of system B ( $\phi_{BR}$ ) are used, and which is expressed as:

$$ROTMAC(\phi_{BRi}, \phi_{Aj}) = \frac{|\phi_{BRi}^T \phi_{Aj}|^2}{(\phi_{BRi}^T \phi_{BRi})(\phi_{Aj}^T \phi_{Aj})} \quad (13)$$

where  $\phi_{Aj}$  is a column vector of the modal matrix  $\phi_A$  and  $\phi_{BRi}$  is a column vector of the modal matrix  $\phi_{BR}$ , obtained rotating matrix  $\phi_B$  as:

$$\phi_{BR} = \phi_B R \quad (14)$$

When using MAC and ROTMAC, no information about changes in scaling can be obtained. Moreover, the rotation effects are eliminated when using  $\phi_{BR}$ ; thus, the ROTMAC is an indicator of shear.

The ROTMAC will be an identity matrix in the following cases:

- System B is perturbed with a stiffness change only ( $\Delta K$ ). This occurs because the rotated mode shapes  $\phi_{BR}$  coincide with mode shapes  $\phi_A$ , indicating no shear effect.
- System B with repeated modes is perturbed with a mass change ( $\Delta M$ ), because in this case, the effect of shear is negligible.

## 3. A SQUARE GLASS PLATE

In this section, the ROTMAC concept is applied to correlate a numerical model with an experimental model of a square laminated glass plate. The plate, measuring 1400 mm x 1400 mm, was composed of two 4 mm thick glass layers and a 1.14 mm polymer interlayer. The plate boundary conditions were pinned at all four corners (Fig. 2).

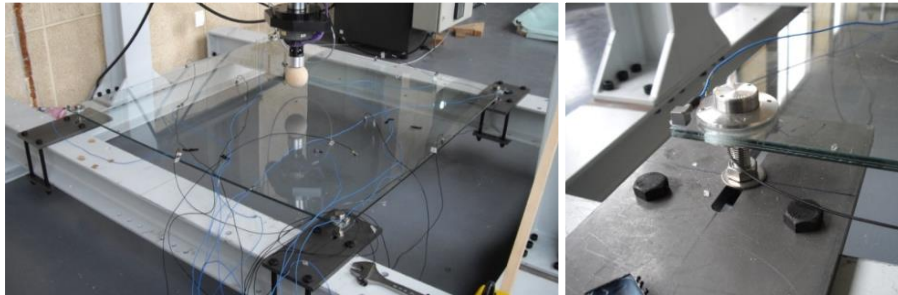


Figure 2. Glass plate and test setup.

The experimental modal parameters were estimated using OMA, which represent the modal parameters of system A. The structure was excited by randomly applying impacts to the plate with an impact hammer. The response was recorded at 25 DOFs using 16 accelerometers with a sensitivity of 100 mV/g.

To cover all 25 DOFs, two data sets were collected with 7 reference sensors. Data acquisition was performed at a sampling rate of 2000 Hz over a duration of 6 minutes. The modal parameters for the first five modes were identified using the EFDD technique. Table 1 presents the experimental natural frequencies, showing that modes 2 and 3 are closely spaced. The experimental mode shapes, normalized to unit length, are illustrated in Fig. 3.

**Table 1.** Experimental and numerical natural frequencies.

Mode	Experimental Freq. [Hz]	Numerical Freq. [Hz]	Error [%]
1	9.35	9.72	3.80
2	19.62	21.11	7.01
3	19.83	21.11	6.10
4	22.53	24.82	9.22
5	55.76	56.11	0.62

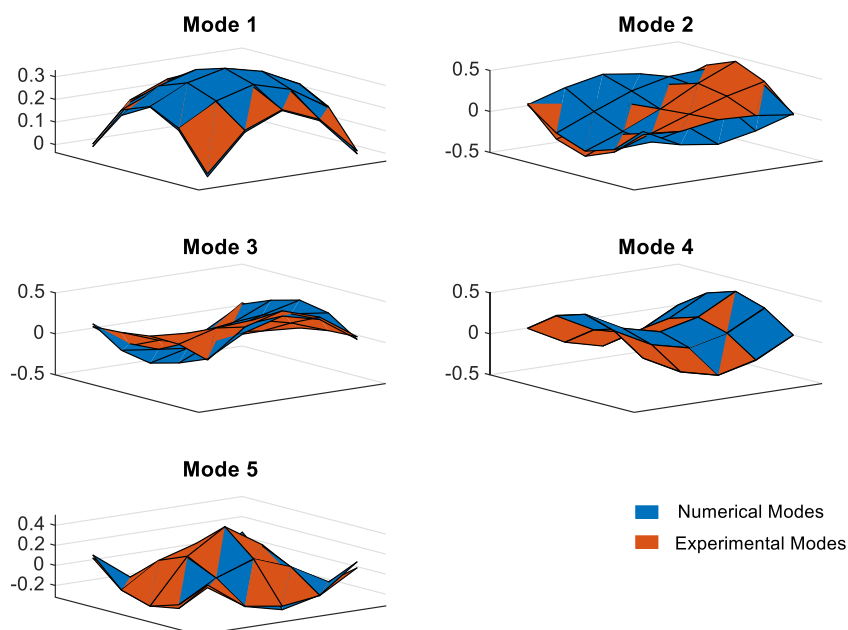


**Figure 3.** Experimental and numerical mode shapes normalized to the unit length.

A 3D finite element model of the structure was previously developed in ANSYS, utilizing a mesh of 19,200 3D quadratic solid elements. The numerical natural frequencies for the first five modes are also presented in Table 1.

The correlation between systems A and B was analysed using the MAC (Fig. 4). The results show that, the values deviate significantly from 1 for modes 2 and 3, suggesting poor correlation. In contrast, modes 1, 4, and 5 exhibit a strong correlation.

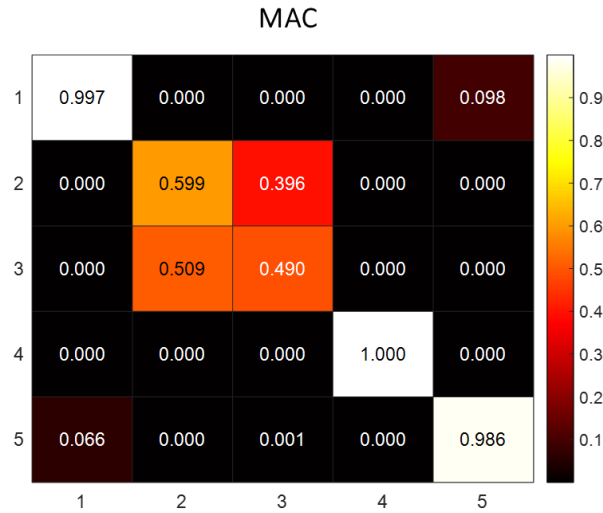


**Figure 4.** Modal assurance criterion between experimental and numerical models.

Considering that experimental mode shapes are unscaled, an estimation of  $T_U$  is obtained with Eq.(7), using five numerical modes and five experimental modes. The matrix  $T_U^T$  is factorized using the QR decomposition, and the resulting  $R$  and  $Q$  matrices are presented in Table 2. From  $R$  matrix a rotation angle of  $-45.5890^\circ$  is obtained for modes 2 and 3, while  $Q$  matrix contains the effects of scaling and shear.

**Table 2.** R (left) and Q (right) matrices.

-0.9992	0.0068	-0.0006	0.0008	0.0390	-1.4819	0.0007	0.0168	-0.0001	-0.0249
-0.0031	-0.6997	-0.7137	-0.0050	0.0330	0.0000	-1.1840	0.1345	-0.0011	-0.0482
0.0056	0.7141	-0.6998	0.0109	0.0084	0.0000	0.0000	-1.1992	-0.0009	-0.0060
0.0007	-0.0113	0.0040	0.9999	-0.0004	0.0000	0.0000	0.0000	-0.9801	-0.0007
-0.0391	-0.0168	-0.0295	-0.0005	-0.9987	0.0000	0.0000	0.0000	0.0000	-1.0596

The 2<sup>nd</sup> and 3<sup>rd</sup> numerical mode shapes are rotated using  $R$  matrix, as shown in Eq. (14), are shown in Fig. 5, together with the respective modes of systems B and A.

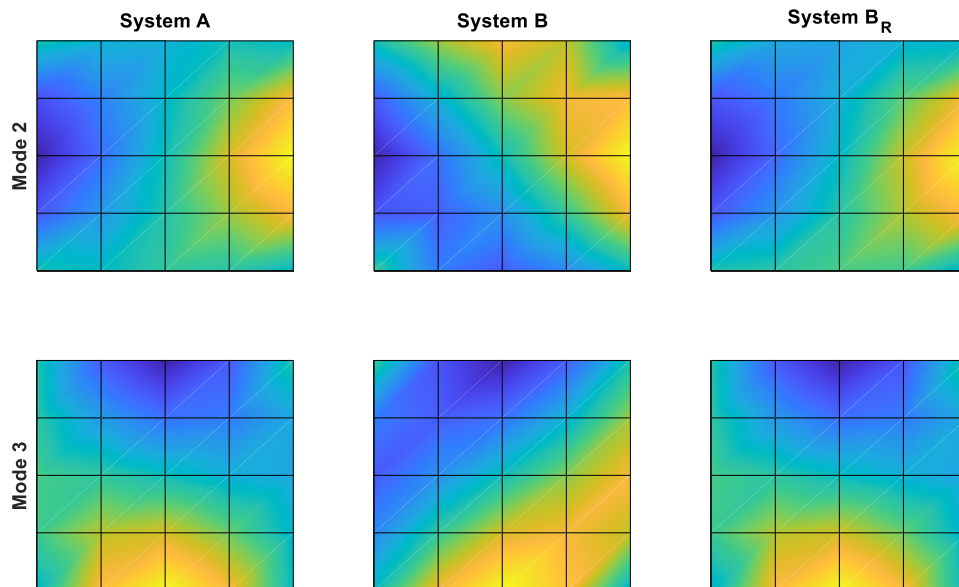


**Figure 5.** Mode shapes 2 and 3 of systems A, B and rotated B ( $B_R$ ).

Moreover, the ROTMAC between the numerical and the experimental models was calculated with Eq. (13), and it is presented in Fig. 6, showing a very good correlation for all modes. The diagonal terms are very close to unity and the off-diagonal terms are very low, indicating that the effect of shear is very low.

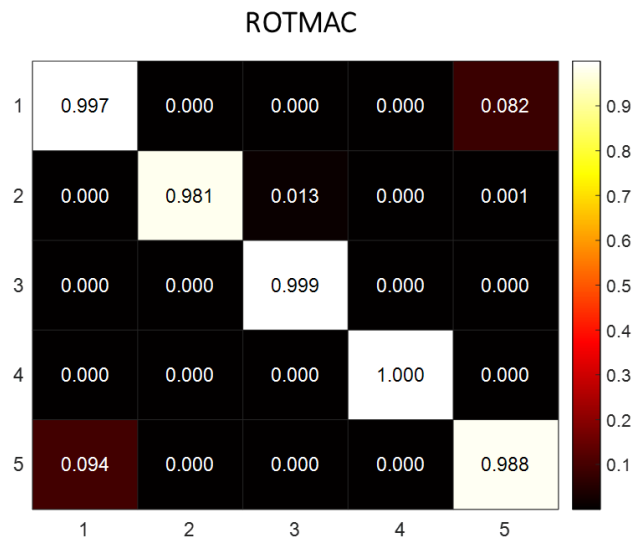


**Figure 6.** ROTMAC: MAC between systems A and B

#### 4. A TWO-STORY THIN LAB STRUCTURE

In this section a lab scale structure of a two-story building is considered to validate the ROTMAC. The structure, made of steel, has two floors of 300 mm x 300 mm and 5 mm thick. The columns have a rectangular section of 5 mm x 5 mm and 800 mm high. The distance between floors is 400 mm.

The modal parameters of the experimental structure are obtained through operational modal analysis (OMA) using eight uniaxial accelerometers with a sensitivity of 100 mV/g (Fig. 7). The test was carried out exciting the structure by hitting it with hands during 9 minutes with a sampling frequency of 2132 Hz. The natural frequencies identified by the SSI-UPC are shown in Table 3 and the mode shapes are shown in Fig. 7. It can be observed that modes 1 and 2 are closely spaced, as well as modes 4 and 5.

**Table 3.** Experimental and numerical natural frequencies.

Mode	Experimental Freq. [Hz]	Numerical Freq. [Hz]	Error [%]
1 (1 <sup>st</sup> bending)	4.18	4.06	2.79
2 (1 <sup>st</sup> bending)	4.29	4.06	5.28
3 (torsion)	7.57	7.37	2.64
4 (2 <sup>nd</sup> bending)	11.16	11.56	3.60
5 (2 <sup>nd</sup> bending)	11.45	11.56	0.98

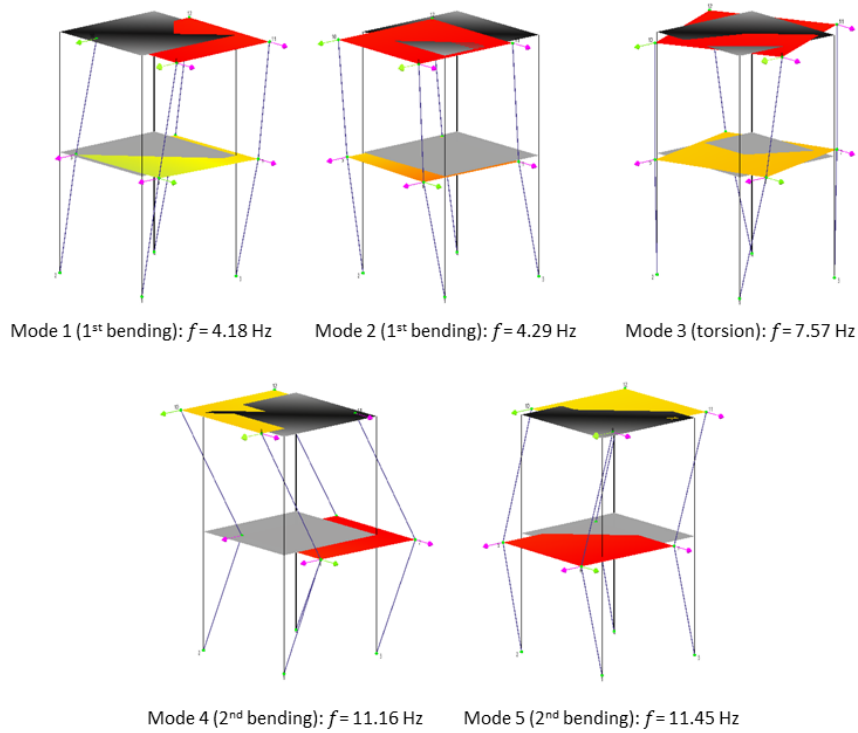


**Figure 7.** Experimental mode shapes

A finite element model of the structure is created in ABAQUS meshing the floors with four nodes shell elements with reduced integration (S4R), whereas the columns were meshed with linear beam elements (B31). The steel was modelled as a linear elastic material with the following mechanical properties:  $E=210$  GPa,  $\rho=7850$  kg/m<sup>3</sup> and  $\nu=0.3$ . The modal parameters were extracted from the FE model through a frequency analysis. The numerical natural frequencies are also shown in Table 3 and the mode shapes in Fig. 8. In this case, modes 1 and 2 are repeated, as well as modes 4 and 5.

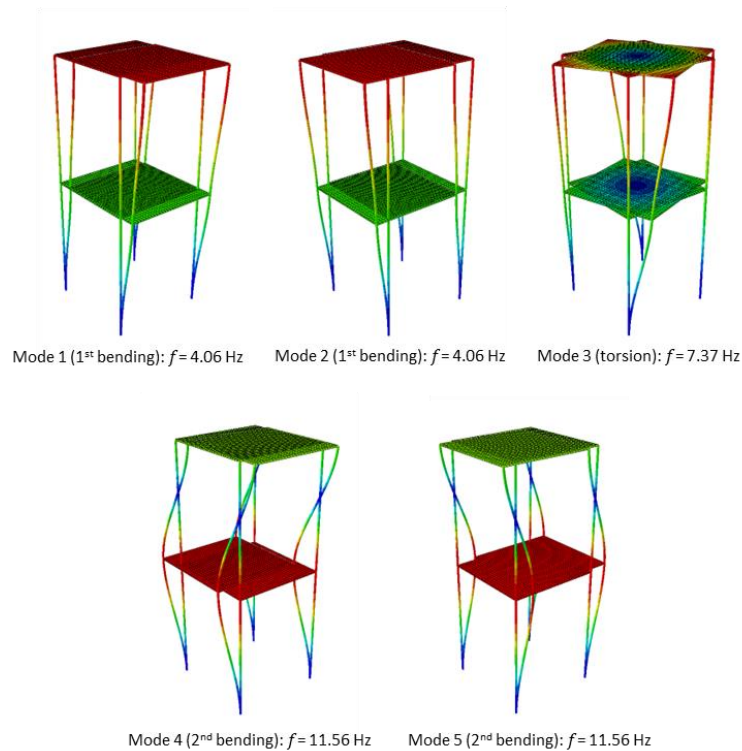


**Figure 8.** Numerical mode shapes

The correlation between the numerical and experimental models is studied through the modal assurance criterion (MAC) shown in Table 4, where it is observed that a good correlation initially exists, with MAC values over 0.96 in the diagonal.

**Table 4.** MAC

0.979	0.002	0.000	0.000	0.000
0.009	0.985	0.000	0.000	0.000
0.000	0.001	0.998	0.001	0.000
0.005	0.000	0.000	0.963	0.023
0.002	0.004	0.000	0.034	0.976

An estimation of matrix  $T_U$  is obtained with Eq. (7), using five numerical modes and five experimental modes, which is factorized using the QR decomposition. The resulting  $R$  and  $Q$  matrices are presented in Table 5. From  $R$  matrix, a rotation angle of approximately  $7^\circ$  is obtained for modes 1 and 2, and an angle of  $12^\circ$  for modes 4 and 5. Fig. 9 presents a top view of modes 1 and 2 for both the experimental and numerical models, indicating that both models move in similar directions.

**Table 5.** R (left) and Q (right) matrices.

-0.993	-0.096	-0.012	0.043	-0.049	2.127	-0.112	0.007	-0.089	-0.163
0.094	-0.991	-0.025	0.032	0.081	0.000	2.326	-0.031	-0.132	0.177
0.012	0.024	-0.999	0.013	-0.029	0.000	0.000	1.861	-0.073	-0.081
-0.049	-0.021	-0.019	-0.981	0.184	0.000	0.000	0.000	-2.345	0.083
-0.048	0.082	-0.025	0.185	0.978	0.000	0.000	0.000	0.000	2.305

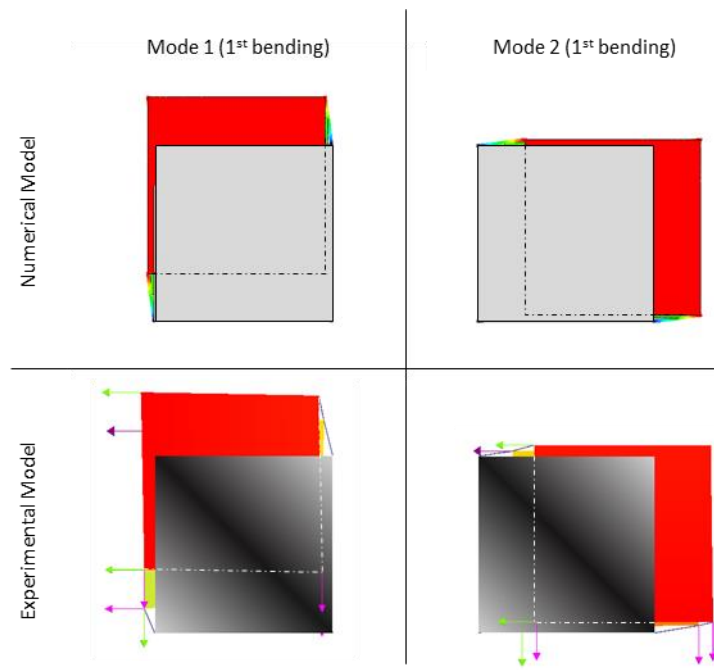


**Figure 9.** Experimental setup and numerical model.

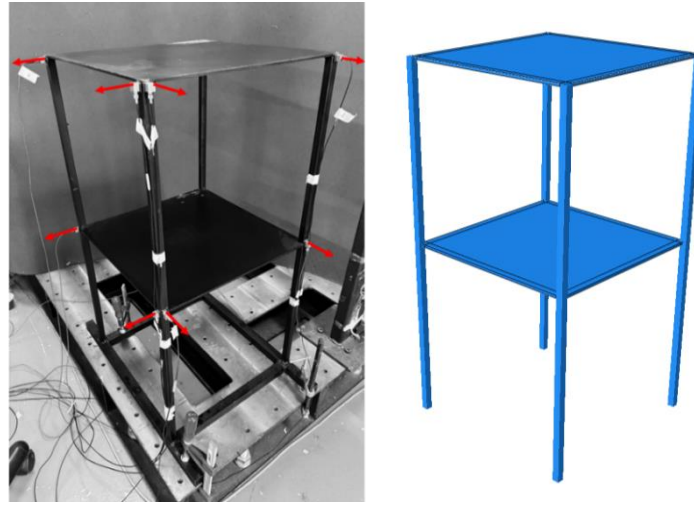
The ROTMAC estimated with Eq. (13) is shown in Table 6, where an improvement of the correlation is observed with all diagonal values over 0.984.

**Table 6.** ROTMAC

0.993	0.002	0.000	0.003	0.005
0.000	0.994	0.001	0.003	0.003
0.000	0.001	0.998	0.001	0.001
0.000	0.000	0.000	0.992	0.001
0.000	0.000	0.001	0.000	0.984

## 5. A TWO-STORY THICK LAB STRUCTURE

In this section another lab scale structure of a two-story building is considered to validate the ROTMAC. The structure, made of steel, has two floors of 400 mm x 400 mm and 5.5 mm thick. The columns have a rectangular section of 15 mm x 15 mm and 800 mm high. The distance between floors is 400 mm.

**Figure 10.** Experimental setup and numerical model.

The modal parameters of the experimental structure are obtained through operational modal analysis (OMA) using eight uniaxial accelerometers with a sensitivity of 100 mV/g (Fig. 9). The test was carried out exciting the structure by hitting it with hands during 4 minutes with a sampling frequency of 2132 Hz. The first five modes were identified by the Enhanced Frequency Domain Decomposition (EFDD) and the corresponding natural frequencies are shown in Table 7.

**Table 7.** Experimental and numerical natural frequencies.

Mode	Experimental Freq. [Hz]	Numerical Freq. [Hz]	Error [%]
1 (1 <sup>st</sup> bending)	14.49	14.81	2.19
2 (1 <sup>st</sup> bending)	14.97	14.81	1.06
3 (torsion)	26.72	25.17	5.81
4 (2 <sup>nd</sup> bending)	59.45	57.25	3.71
5 (2 <sup>nd</sup> bending)	60.77	57.25	5.80

Moreover, a finite element model of the structure is created in ABAQUS. The floors were meshed with four nodes shell elements with reduced integration (S4R), whereas the columns were modelled with linear beam elements (B31). The steel was modelled as a linear elastic material with the following mechanical properties:  $E=210$  GPa,  $\rho=7850$  kg/m<sup>3</sup> and  $\nu=0.3$ . The natural frequencies extract from the FE model through a frequency analysis are shown in Table 7.

The MAC between the numerical and experimental models is Table 8.

**Table 8.** MAC

0.856	0.156	0.000	0.015	0.003
0.143	0.843	0.000	0.001	0.010
0.001	0.001	0.999	0.001	0.000
0.013	0.002	0.000	0.909	0.092
0.000	0.013	0.000	0.090	0.905

From Table 8 it is inferred that there is a very good correlation in mode 3 (torsional), but a poorer correlation has been achieved in the bending modes (MAC values of 0.856 and 0.843 for modes 1 and 2, and 0.909 and 0.905 for modes 4 and 5).

An estimation of  $T_U$  is obtained using Eq. (7), and the  $R$  and  $Q$  matrices are derived through the QR decomposition, as shown in Table 9. From these matrices, it is inferred that modes 1 and 2 rotate by  $22.3^\circ$ , while modes 4 and 5 rotate  $17.5^\circ$ .

**Table 9.** R (left) and Q (right) matrices

-0.925	0.379	-0.022	-0.003	0.013	-3.083	-0.052	0.028	0.050	0.057
-0.379	-0.925	0.011	0.004	-0.003	0.000	3.122	0.066	-0.060	-0.027
0.016	-0.019	-1.000	-0.016	-0.008	0.000	0.000	2.916	0.000	-0.043
0.004	-0.006	0.013	-0.953	0.301	0.000	0.000	0.000	-3.325	-0.005
0.010	-0.007	-0.012	0.301	0.953	0.000	0.000	0.000	0.000	3.305

The ROTMAC calculated with Eq. (13) is presented in Table 10, where it can be seen that the correlation between the numerical and experimental models is very high, thus no shear effects are observed.

**Table 10.** ROTMAC

1.000	0.000	0.000	0.016	0.000
0.000	0.999	0.001	0.000	0.014
0.000	0.000	0.999	0.000	0.000
0.013	0.000	0.000	0.999	0.000
0.000	0.012	0.000	0.000	0.996

## 6. CONCLUSIONS

In summary, the following conclusions can be drawn:

- The ROTMAC concept has been validated through three applications cases with closely spaced mode shapes, where the correlation between an experimental and a numerical model has been studied.
- A square glass plate with two closely spaced modes with a local rotation angle of  $45.6^\circ$  was presented. The ROTMAC show a huge correlation between the numerical and the experimental model, even that the MAC values were very low.
- A two-story thin lab structure was also studied. The initial correlation in term of MAC was significantly good, with lowest value been 0.963. Although very low local rotations were obtained, a slight improvement in the ROTMAC values in comparison to the MAC was achieved.

- Another two-story lab structure with bigger stiffness was studied. In the case, two local rotations of  $22.3^\circ$  and  $17.5^\circ$  were obtained. The obtained ROTMAC values show a very strong correlation between the numerical and experimental model.
- The effect of local rotations has been successfully eliminated by the use of the ROTMAC, and the correlation in symmetric structures can be successfully studied.

## ACKNOWLEDGEMENTS

The authors would like to express their gratitude to the Spanish Ministry of Science and Innovation for the financial support through the following projects: MCI-20-PID2019-105593GB-I00/AEI/10.13039/5011000-11033, MCI-21-PRE2020-094923, and PID2023-147535OB-I00 funded by MCIU/AEI/10.13039/501100011033 and by FEDER, EU.

## REFERENCES

- [1] A. Sestieri and W. D'Ambrogio. A modification method for vibration control of structures. *Mech. Syst. Signal Process.* 3 229–253, [https://doi.org/10.1016/0888-3270\(89\)90051-4](https://doi.org/10.1016/0888-3270(89)90051-4), 1989.
- [2] Avitabile P. Twenty years of structural dynamic modification - A review. *Sound and Vibration*, 2003.
- [3] M. Aenlle, García-Fernández, N. and F. Pelayo. Rotation of mode shapes in structural dynamics due to mass and stiffness perturbations *Mech. Syst. Signal Process.* 112 111269. <https://doi.org/10.1016/j.ymssp.2024.111269>, 2024.
- [4] C.R. Goodall, Computation using the QR decomposition, in: *Handb. Stat.*, 1993: pp. 467–508. [https://doi.org/10.1016/S0169-7161\(05\)80137-3](https://doi.org/10.1016/S0169-7161(05)80137-3).